Title
Resist requirements and limitations for nanoscale electron-beam patterning

Authors
Liddle, J. Alexander
Gallatin, Gregg M.
Ocola, Leonidas E.

Publication Date
2002-11-25

Resist Requirements and Limitations for Nanoscale Electron-Beam Patterning

J. Alexander Liddle,[1] Gregg M. Gallatin[2] and Leonidas E. Ocola[3]
[1]Materials Sciences Division, Lawrence Berkeley National Laboratory
Berkeley, CA 94720, USA
[2]IBM T.J. Watson Research Center
Yorktown Heights, N.Y. 10598, USA
[3]Advanced Photon Source, Argonne National Laboratory
Argonne, IL 60439, USA

ABSTRACT

Electron beam lithography still represents the most effective way to pattern materials at the nanoscale, especially in the case of structures, which are not indefinitely repeating a simple motif. The success of e-beam lithography depends on the availability of suitable resists. There is a substantial variety of resist materials, from PMMA to calixarenes, to choose from to achieve high resolution in electron-beam lithography. However, these materials suffer from the limitation of poor sensitivity and poor contrast.

In both direct-write and projection e-beam systems the maximum beam current for a given resolution is limited by space-charge effects. In order to make the most efficient use of the available current, the resist must be as sensitive as possible. This leads, naturally, to the use of chemically amplified (CA) systems. Unfortunately, in the quest for ever smaller feature sizes and higher throughputs, even chemically amplified materials are limited: ultimately, sensitivity and resolution are not independent. Current resists already operate in the regime of < 1 electron/nm^2. In this situation detailed models are the only way to understand material performance and limits.

Resist requirements, including sensitivity, etch selectivity, environmental stability, outgassing, and line-edge roughness as they pertain to, high-voltage (100 kV) direct write and projection electron-beam exposure systems are described. Experimental results obtained on CA resists in the SCALPEL® exposure system are presented and the fundamental sensitivity limits of CA and conventional materials in terms of shot-noise and resolution limits in terms of electron-beam solid interactions are discussed.

INTRODUCTION

Some years ago it was still possible to treat the resist requirements for high sensitivity and high resolution as two separate cases, divided between commercial applications, such as mask making, and small scale patterning for research. More recently, however, the separation between these two domains has all but disappeared. This has been driven primarily by the continuing reduction in feature size accompanying the progress of the semiconductor industry (Figure 1). The concomitant demands on mask fabrication have become rigorous, particularly with the introduction of sub-resolution elements for optical proximity effect correction [1]. In addition, as optical lithography becomes more difficult and costly, there is a strong possibility that electron-beam systems will be used directly [2, 3] for the mass production of integrated circuits (IC's). These factors mean that electron-beam resists are now required to provide high resolution and high speed simultaneously.

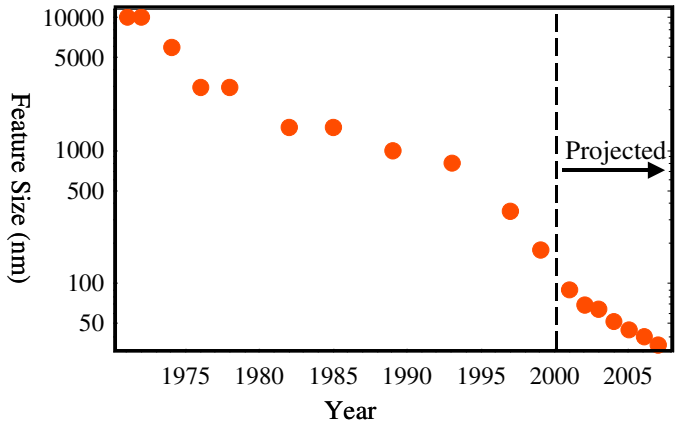

Figure 1. Minimum integrated circuit feature size as a function of time.

In this paper we will discuss the detailed requirements for advanced electron-beam resists, review the basic mechanisms governing resist exposure and development with particular attention to the statistics of the processes involved, and, finally, consider what the fundamental limitations to the resolution of electron-beam lithography might be.

RESIST REQUIREMENTS

Process stability

Process stability covers a number of specific factors related to variations in the printed feature size or critical dimension (CD). The overall CD tolerance is usually given as ±10%, with process related effects allowed to contribute only ±3%.

Table I. Values of process sensitive parameters for electron-beam resists.

Process Sensitive Parameter	Value
Post Exposure Delay (PED) Time	> 3 hrs
Development Time	< 5% CD/minute
Etch Resistance	= Polyhydroxystyrene
Post Exposure Bake (PEB)	< 1% CD/°C
Developer	0.26N TMAH
Vacuum Compatibility	Zero outgassing

The requirements in Table I are generic for all lithographic technologies, apart from the need for vacuum compatibility. The evolution of volatile organic compounds from the resist while it is in the electron-beam system is highly undesirable because of the potential for contamination of the electron-optical column with material that can charge and degrade the system performance. In addition, the loss of material from the resist can adversely affect the resist performance.

In a single component material, such as PMMA, solvent can escape from the film, but this can be addressed using a suitable pre-exposure bake protocol. However, particularly in view of the indiscriminate nature of the radiolysis induced by electron-beam exposure, there is always the potential for the production of volatile moieties – in the case of PMMA substantial amounts of MMA monomer are evolved.

Chemically amplified materials contain a base resin with pendant protecting groups (positive tone), or a cross-linker (negative tone), in addition to a base, a photoacid generator (PAG), residual solvent, as well as additives to promote adhesion and film formation. During exposure a latent image of acid is formed in the film. The acid then goes on to catalyze a number of deprotection or cross-linking reactions (Figure 2).

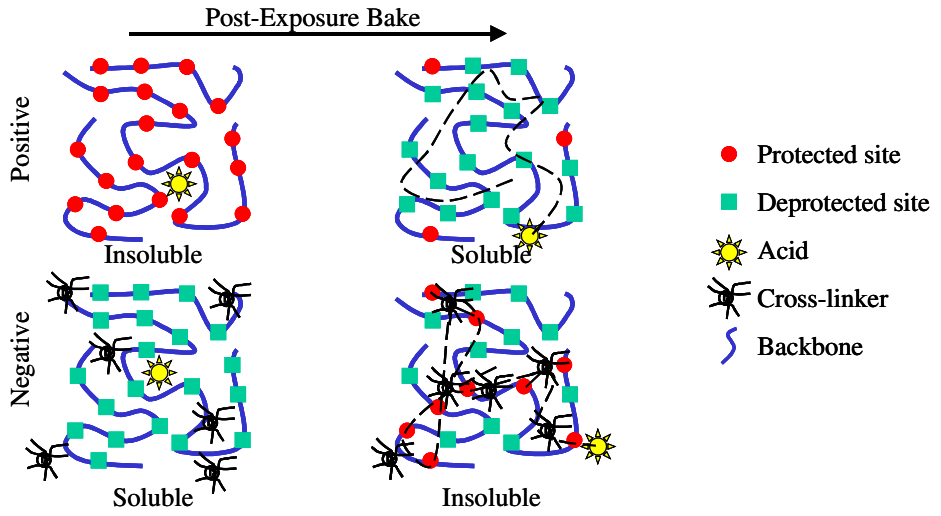

Figure 2. a) Schematic of the exposure mechanism for a CA resist [7]. Note that the crosslinker functions to protect soluble sites, rather than link polymer chains.

Loss of the PAG from the film, which could be exacerbated by the vacuum environment, will obviously degrade the lithographic performance of the resist, which suggests that large molecules that can associate with the polar functionalities of the resist are required. Ideally the acid formation process should not occur through a reaction involving leaving groups, and the acid molecule itself should be large enough to be non-volatile. It is also important that either the kinetics of the acid catalyzed reaction is minimal at the maximum temperature the resist experiences in the exposure system, which requires that it be a high activation energy (E_a) process, or that the volatility of the products is zero. Current experience suggests that the high E_a materials are most suitable.

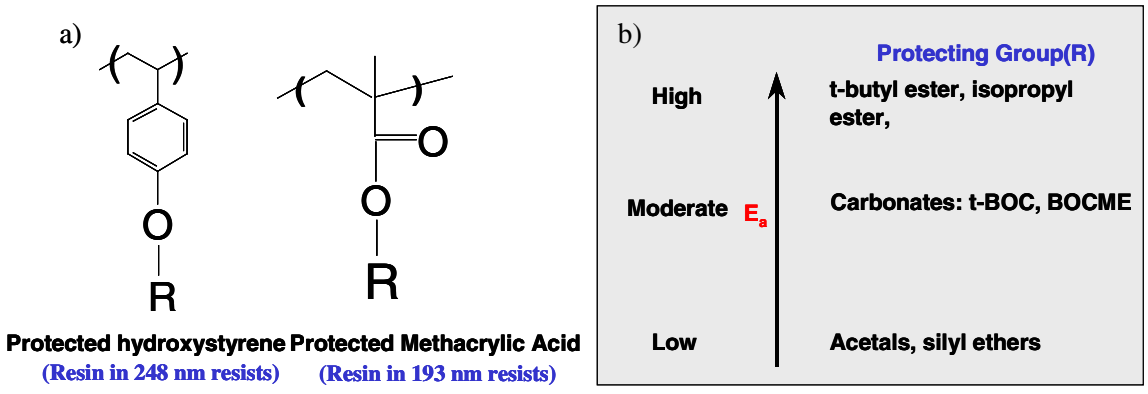

Figure 3. a) Typical resist structures for 248 nm and 193 nm resists, which are also suitable for electron-beam systems. b) Influence of protecting group, R, on activation energy for deprotection reaction.

It is important to note that the absorption or optical density is not an issue for electron-beam resists. This imposes a major constraint on the design of optical resists because the transparency of the materials needs to be adjusted so that the absorption through the film thickness does not lead to excessive resist sidewall angles due to depth variation of the deposited energy profile [4]. This is becoming harder to realize as the exposure wavelengths used decrease from 248 nm to 193 nm and below as fewer and fewer polymer systems are available with acceptable absorption characteristics. Limitations on the choice of polymer components can also affect the etch resistance of the material, which is influenced by its fractional carbon content, and by the relative proportion of carbon atoms contained within a ring structure [5,6].

Contrast

The resist contrast is a measure of how non-linear the response of the development process is to the chemical contrast produced in the material after exposure and is essential in determining how small an image modulation can be successfully converted into an actual developed resist image. A typical requirement for conventional IC manufacture is that the contrast should exceed 5, but there is no upper limit, greater values leading to steeper sidewall angles. Note, however, that if topographic control of a resist surface is desired, as in the production of diffractive optical elements, then low contrast values are useful.

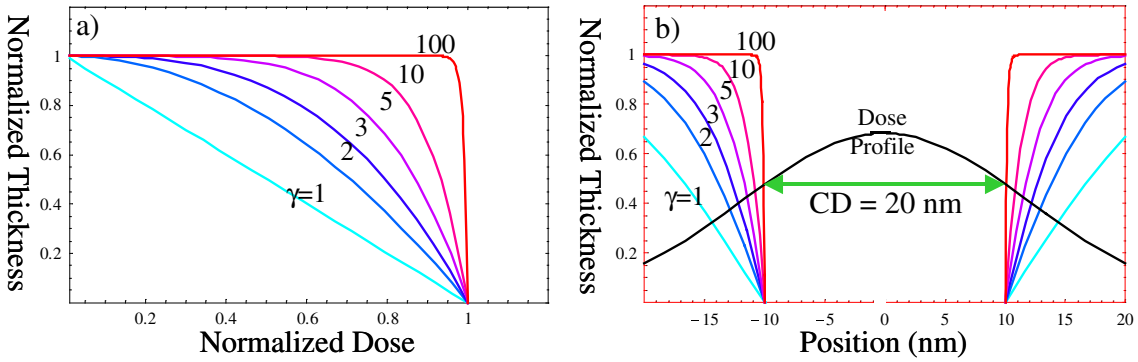

Figure 4. a) Normalized film-thickness remaining versus normalized dose for a positive resist material for different values of the dissolution rate contrast, γ, defined as $\gamma = \frac{d \ln r}{d \ln E}$, where r is the dissolution rate from an exposure dose E. b) Normalized film-thickness remaining versus position for a 20 nm feature printed with a 10 nm σ Gaussian blur (Dose Profile) for different values of the contrast, γ, assuming uniform energy deposition through the film thickness.

The contrast is determined by the nature of the development process. In a non-chemically amplified material, such as PMMA, the effect of exposure is to cause scissioning of the main polymer chain. The developer used is a minimal solvent for the material, and it extracts the lower molecular weight polymer chains from the exposed regions more rapidly than the high molecular weight chains from the unexposed regions leading to a variation in dissolution rate with dose. This is a process that is strongly

dependent on kinetics, and, since it is essentially sorting material on the basis of molecular weight differences, it is fundamentally a low contrast process.

Certain measures can be taken to improve the contrast, such as reducing the polydispersivity (the ratio of the weight average to number average molecular weight) of the starting polymer. If the polydispersivity is small, then it is easy to establish a clear separation in weight distribution between exposed and unexposed areas. This also has the effect of reducing the dose necessary to achieve that separation.

In a chemically amplified material, there is a change in polarity between the exposed and unexposed areas. In a positive tone material, exposure results in the conversion of an insoluble non-polar material into a highly soluble polar material. The change in solubility occurs when the density of deprotected sites exceeds a critical value and is relatively abrupt [7]. Aside from the change in solubility, this process converts the material from hydrophobic to hydrophilic, which further encourages the attack of the developer on the exposed regions. These factors lead to CA resists having typically very high contrasts.

Sensitivity

Reductions in exposure dose have been essential in making technologies such as 248nm and 193nm optical lithography and electron-beam mask making systems viable, in terms of throughput, because of limitations in the sources. Mask making has, until recently, relied on simple post-processing of the resist image – wet Cr etching – and so the demands on the resist have been minimal in terms of its process robustness. These demands have been satisfied with single component materials such as PBS [8] and COP [9], which were optimized primarily for sensitivity. Optical resists have had to meet all the demands of IC fabrication and so have developed as complex systems with a number of components that offer the ability to optimize sensitivity as well as features such as etch resistance and process stability independently [10]. These considerations have naturally led to the chemically amplified (CA) resist systems developed for optical lithography finding application in electron-beam systems.

In electron beam systems for IC manufacture, low doses are critical for a number of reasons. Resolution in electron-beam systems is linked to the beam current through the space-charge effect: electron-electron interactions in the beam cause blurring of the image, which increases as the beam current is increased [11, 12]. The development of a more sensitive material can therefore be of benefit in two ways: for a fixed beam current the throughput can be increased, or, for a given throughput, the beam current can be decreased and the resolution improved. In addition to the tradeoff between resolution and throughput, heating, both of the wafer and the mask, is reduced as the sensitivity improves. High-throughput systems typically operate at 100 kV and at beam currents as high as 30 μA; a heat load of 3 W deposited deep in the wafer. For example, a 10 $\mu C/cm^2$ dose requirement will lead to an overall wafer temperature increase of about 8 K: the heating process is of course localized to the beam and thus leads to dynamic wafer distortions that can be a significant contributor to the total overlay error [13,14].

Fortunately there is some relief from the requirement to continue endlessly reducing the sensitivity. The system throughput depends on other factors such as stage speed, alignment time and wafer load/unload overhead, which means that there is little to be gained in throughput once the exposure time becomes much less than the system

overhead time. Similarly, the resolution is ultimately limited by electron-optical aberrations, and there is a point at which further reductions in beam current will not improve resolution. These factors mean that there is a practical lower limit on the minimum sensitivity required, which will vary with the system design details, however, values as challenging as 1 $\mu C/cm^2$ [15] have been specified.

It should be noted that similar considerations apply in direct write systems, particularly mask making tools. In such systems the minimum useful sensitivity is determined by the beam current and the deflection speed. For example, in a raster scanning mask maker with a deflection speed of 320 MHz, a maximum beam current of 720 nA and a pixel size of 120 nm, the minimum useful resist sensitivity is 16 $\mu C/cm^2$ [1]. A typical vector beam tool for nanolithographic applications [16] operating at 25 MHz with a beam current of 500 pA and a pixel size of 8 nm would be able to employ a resist with a sensitivity as low as 31 $\mu C/cm^2$, while very high resolution work, which might need a pixel size of 2 nm, would increase this value to 500 $\mu C/cm^2$.

IC Manufacture vs Nanofabrication

Although the feature sizes involved in IC manufacture are starting to approach the nanoscale domain, there are a number important differences between the respective resist requirements. First, sensitivity: this is not, within reason, a major concern for the nanofabrication community, where the resolution is the dominant performance metric, whereas for IC production where overall manufacturing costs are very strongly weighted by throughput, it is critical. Second, the evolution of volatile products from the resist film can be tolerated to a limited extent in nanofabrication, because the very low typical throughputs mean that the total volume of material released into the vacuum system is small. Third, the requirement for compatibility with a TMAH developer can be relaxed since the use of different developers, including organic solvents, is only an issue in the context of the large quantities needed in a production environment.

Resolution

So far we have not discussed the resolution requirement, since this is intimately linked to both the contrast and sensitivity through the details of the image formation process. We now consider those details in the context of their effect on the ultimate resolution attainable. Note that we judge the resolution limit to be defined by the smallest equal lines and spaces that can printed. Smaller isolated features are always possible, but are more representative of the process than the resist.

Aerial Image

Calculation of the aerial image in an electron-beam system is relatively straightforward because diffraction effects are negligible at the short (3.7 pm at 100 keV) wavelengths used. This means that the convolution of a suitable point-spread function (PSF) with the desired features is sufficient [17].

In a high-throughput system, such as a mask-writer or projection tool, the PSF is comparable in size to the features being printed, in order to maximize the beam current, which means it has a substantial impact on the ultimate resolution and process latitude.

The situation is somewhat different for nanofabrication systems where the PSF can be much smaller than the feature ranging from a Gaussian with a σ of 5 nm for commercial tools to 0.5 nm in systems based upon scanning transmission electron microscopes.

Figure 5 shows the aerial image for 20 nm features at several different Gaussian blur values.

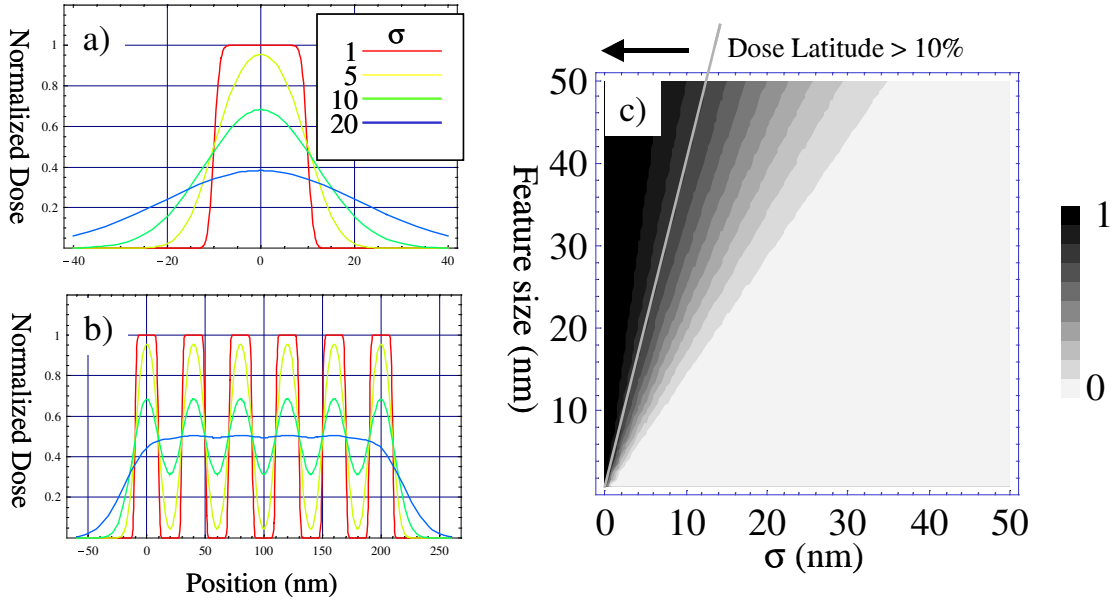

Figure 5. Aerial image intensity profiles for isolated and dense features as a function of Gaussian beam blur width, σ. a) 20 nm isolated feature, b) 20 nm lines and spaces, c) Normalized modulation transfer function as a function of feature size and blur.

Once the blur reaches roughly $\sqrt{2Ln2}$ of the feature size the aerial image contrast becomes negligible, hence, in the ideal case of infinite resist contrast and no other sources of blur, the resolution attainable is determined solely by the beam blur. It is necessary, however, to provide some latitude in the process. If we define an acceptable variation in dose as one that causes less than a 10% change in the feature size, then the blur should be less than 20% of the feature size.

Statistics

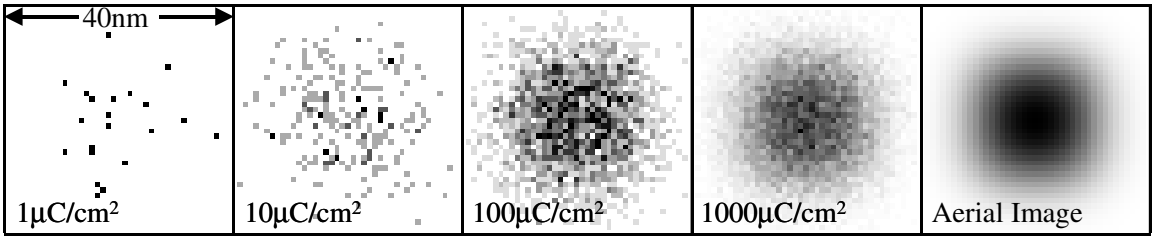

Figure 6. Arrival statistics for a 20 nm square feature printed with a Gaussian blur of 5 nm σ at doses of 1, 10, 100 and 1000 μC/cm^2 respectively. 1000 μC/cm^2 corresponds to an average of 62.5 electrons/nm^2. The gray level in each pixel corresponds to the number of electrons arriving in a 1 nm square.

Unfortunately the aerial images shown above really only represent the probability of finding an electron at a particular location. The low doses demanded for high throughput mean that the number of electrons delivered is small enough that the arrival statistics can cause dose variations (Figure 6) that could, in principle, lead to significant feature size variations [18, 19].

The most basic limit to the resolution from a statistical perspective is given by the mean separation between the electrons, and corresponds to $4\ nm/\sqrt{S}$, where S is the sensitivity in μC/cm^2, leading to dose of 16 μC/cm^2 or 1 e$^-$/nm^2 for 1 nm resolution. Note that this approach does not include the three dimensional nature of the exposure. A more realistic value is obtained through making a signal to noise argument and requiring that the uncertainty in the dose within a resolution element be less than 10%, for example, giving a dose value of 1600 μC/cm^2 for the same resolution. Exactly what the limit is will be controlled by what constitutes a meaningful resolution element. Clearly the molecular size of the resist is one such limit, while the maximum tolerable value of the line edge roughness, typically 10% of CD, is another. We could also choose the CD, and, bearing in mind that for an isolated feature the dose to print on size is twice the threshold dose for development, calculate the probability that the dose falls below threshold so that the feature fails to print. If we choose an error threshold of 1 in 10^{15}, the minimum dose is approximately 200 particles per feature, corresponding to a dose of 32 μC/cm^2 for a 10 nm square feature. As Figure 7 shows, the most sensitive resists are operating well at 5 – 6 μC/cm^2 for 100 nm features, so the simple square law scaling derived from any of the above criteria would indicate that the worst case required sensitivity at 20 nm should be no more than 125 - 150 μC/cm^2.

We should note at this point, that the arrival statistics do not constitute the whole story. In a 100 nm thick resist film each 100 keV electron is on average responsible for an average of one ionization event. As we will discuss shortly, these events are not localized, and naturally lead to some smoothing out of the arrival statistics.

In the case of CA resists, the simple statistical picture would seem to be rather damning in terms of the likely resolution because of the small volume fraction that the photoacid generator molecules occupy. This would lead one to imagine that the number of electrons necessary would have to be increased to account for the reduced probability of a "hit" on a PAG molecule.

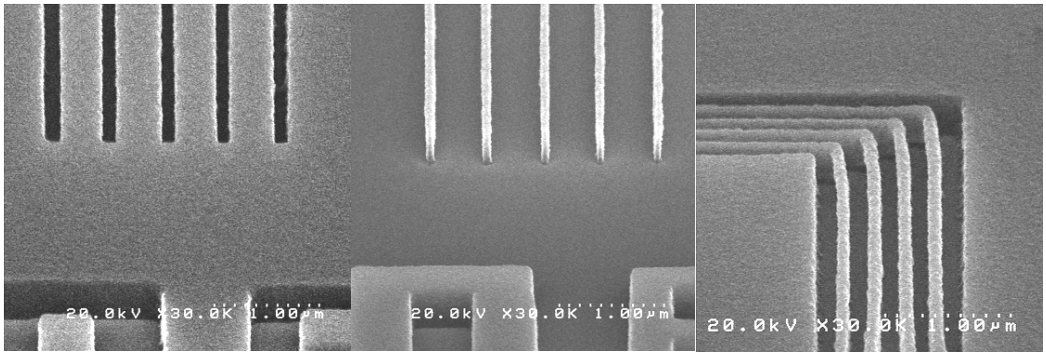

80 nm, 5.8 μC/cm^2 80 nm, 5.8 μC/cm^2 100 nm, 5.4 μC/cm^2

Figure 7. Results obtained from chemically amplified resist (TOK EP004, positive, and EN009, negative) exposed on the SCALPEL® system.

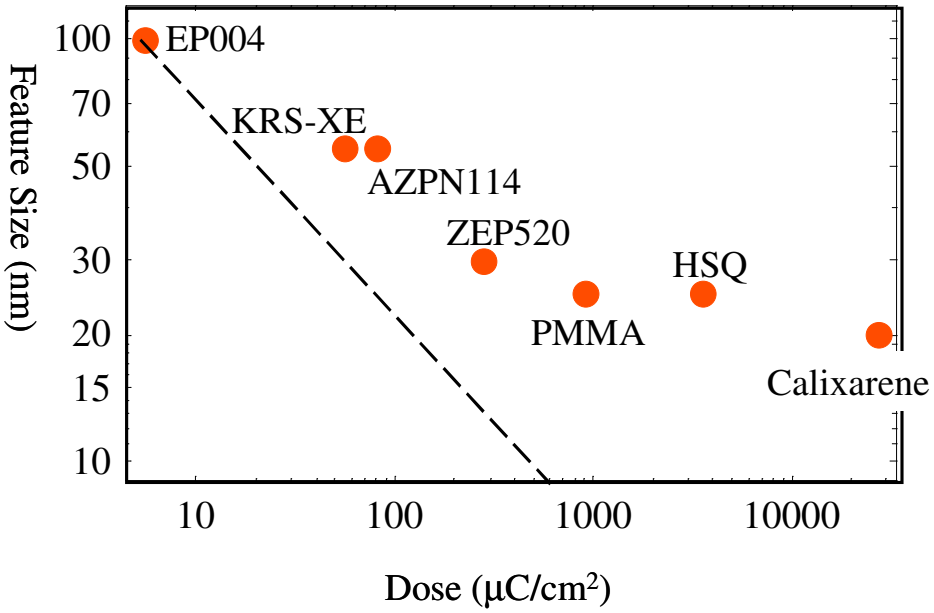

Figure 8. Resolution versus process dose for a range of resists for equal lines and spaces. The dashed line represents the Dose$^{-1/2}$ dependency that we would expect to observe, scaled to EP004 at 5.8 μC/cm^2.

Recent work [20, 21], however, has suggested that ionization events in the base polymer can also result in acid generation through an electron "scavenging" process, substantially increasing the efficiency with which incident electrons are converted into acid species.

The situation in CA materials increases in complexity when one considers the role of acid diffusion and its effect on the developed image. Image formation in CA materials can be thought of as a concatenation of statistics - dose – acid formation – PEB chemistry – dissolution rate – surface evolution – and can be modeled as such [22]. The net result is that the initial dose statistics are washed out [22]. Detailed models have been produced of the processes occurring during acid diffusion and acidolysis [23, 24, 25], incorporating effects such as the sharp decrease in acid diffusion that occurs when the acid is diffusing in a deprotected as opposed to protected area and the evolution of deprotected site density during post-exposure bake. Current estimates [26] put the acid diffusion range at 5 nm during a typical post exposure bake, indicating that it is the highly efficient acidolysis process that is a major cause of image blur during PEB at large feature sizes, while the two are equally important in the 40 – 50 nm range, with acid diffusion dominating at the smallest feature sizes.

Energy deposition distribution

We can see from Figure 8 that the resolution that can be obtained ceases to improve as the dose continues to increase: at this juncture it is appropriate to consider how the energy of the incident electron beam is actually distributed through the resist. If we confine ourselves to a discussion of high-energy (> 50 keV) electrons, then forward scattering is a negligible factor in controlling the form of the deposited energy profile [27,28], as expected. 90% of a 100 keV beam is contained within a diameter of 8 nm at the base of a 100 nm thick resist [28]. The bond-breaking that accompanies the passage

of the incident electron is controlled by the distribution of ionization events, plasmons and the trajectories of electrons generated within the resist [29]. We note that the peak in the secondary electron energy distribution is approximately 10 eV [25], and that such low energy electrons can have mean free paths of several nanometers [30]: these factors, combined with the "scavenging" picture [21], requires that these low energy electrons be accounted for carefully in CA materials. We note that it has been suggested that the PAG, through the scavenging effect, limits the range of thermalized electrons [20, 21]. Figure 9 shows the results of a simulation that does so, and indicates that the beam broadening in the resist as a consequence of these processes is approximately 10 nm. This result suggests that there is little to be gained by reducing the incident beam blur much beyond 5 nm.

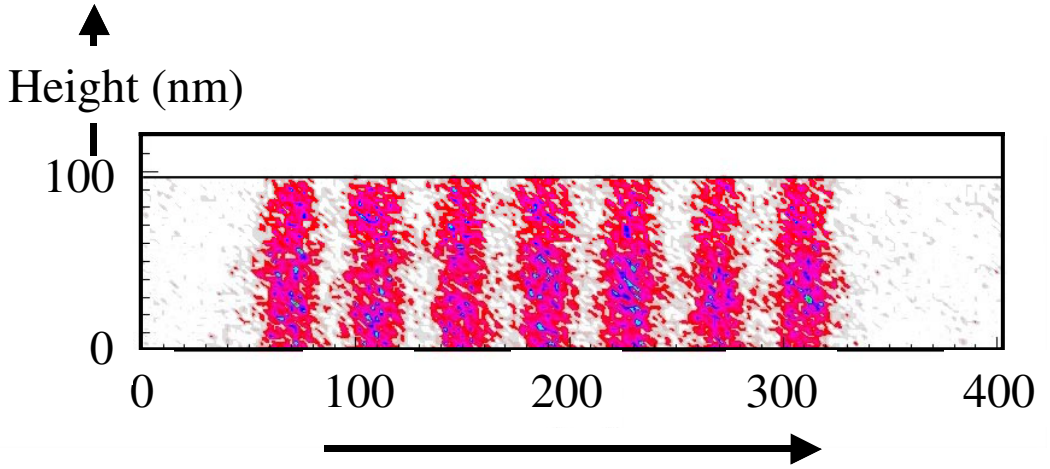

Figure 9. Deposited energy distribution in a 100 nm thick resist for a square-wave function (20 nm lines and spaces) incident beam generated using a Monte-Carlo simulation of a 20 μC/cm^2 dose.

PERFORMANCE LIMITS

From the preceding discussion it is clear that the minimum feature size is ultimately controlled by the energy deposition profile. It should be noted that there are instances where higher resolution has been achieved using electron-beam systems and inorganic resists such as SiO_2 [31] and Al_2O_3 [32, 33]. The exposure mechanism in these cases involves high energy-loss events, which therefore tend to be highly localized. In the case of SiO_2 radiation damage occurs by knock-on, while in Al_2O_3 feature formation proceeds through lattice defect production at very high rates in a process that relies upon the excitation of core electrons, necessitating the use of very high current densities and doses in the C/cm^2 range. Though interesting, such methods cannot form the basis of a viable nanofabrication technology.

CONCLUSIONS

The resolution that can be obtained in an electron-beam resist is limited by the modulation in the deposited energy profile that can be generated. This means that features below about 20 nm (lines and spaces) cannot be resolved in conventional organic resist materials – indicated by the fact that the smallest features produced have not been

bettered in almost three decades [34, 35]. However, the ease of producing those features can be greatly enhanced by the increasing the resist contrast to take full advantage of whatever dose latitude may be available. In addition, if dose is not a constraining requirement, then we might expect that the feature quality (i.e. LER) would improve [36] based upon signal-to-noise arguments. These considerations suggest that CA materials with their high-contrast development mechanisms will become increasingly useful for high resolution work, especially if the formulations are changed to benefit from relaxations in, for example, the amount of PAG that can be incorporated or the absence of a need for optical transparency [37], and to reduce diffusion lengths and catalytic chain lengths to match the lower required sensitivities. Recently, novel resists based on hybrid organic/inorganic nanocomposites have been developed and show some indications of improved resolution, possibly through a reduction in the fast secondary range [38].

ACKNOWLEDGEMENTS

The authors would like to acknowledge F.A. Houle, W.D. Hinsberg, J.M.M. Macaulay and A.E. Novembre for helpful discussions. This work was supported in part by DARPA under contract number MDA972-98-C-0007 and by the Director, Office of Science, Office of Basic Energy Sciences, Materials Science and Engineering Division, U.S. Department of Energy under Contract Nos. DE-AC03-76SF00098 and W-31-109-ENG-38.

REFERENCES

1. F. Abboud , Ki-Ho Baik, V. Chakarian, D. Cole, J. Daniel, R. Dean, M. Gesley, Maiying Lu, R. Naber, T. Newman, F. Raymond, D. Trost, M. Wiltse, W. DeVore, Proc. SPIE **4562**, 1 (2002).
2. J.A. Liddle, L.R. Harriott and W.K. Waskiewicz, Microlithography World, **6**, 15 (1997).
3. S. D. Golladay, H. C. Pfeiffer, J. D. Rockrohr, and W. Stickel, J. Vac. Sci. Technol., **B18**, 3072 (2000).
4. R.L. Brainard, G.G. Barclay, E.H. Anderson, L.E. Ocola, Microelectronic Engineering, **61-62**, 707 (2002)
5. Y. Ohnishi, M. Mizuko, H. Gokan and S. Fujiwara, J. Vac. Sci. Technol., **19**, 1141 (1981).
6. R. Kunz et al., Proc. SPIE **2724**, 365 (1996).
7. L.E. Ocola, to appear in J. Vac. Sci. Technol., Proceedings of the 46th EIPBN meeting.
8. M.J. Bowden, L.F. Thompson and J.P. Ballantyne, J. Vac. Sci. Technol., **12**, 1294 (1975).
9. L.F. Thompson, J.P. Ballantyne and E.D. Feit, M.J. Bowden, L.F. Thompson and J.P. Ballantyne, J. Vac. Sci. Technol., **12**, 1280 (1975).
10. R.D. Allen, W.E. Conley and R.R. Kunz, in *Microlithography, Micromachining and Microfabrication*, edited by P. Rai-Choudhury (SPIE Optical Engineering Press, Bellingahm, 1997), p. 321.
11. M. M. Mkrtchyan, J. A. Liddle, S. D. Berger, L. R. Harriott, J. M. Gibson and A. M. Schwartz, J. of Appl. Phys., **78**, 6888 (1995).

12. M. M. Mkrtchyan, J. A. Liddle, S. T. Stanton, E. Munro, W. K. Waskiewicz, Microelectronic Engineering, **53**, 299 (2000).
13. N. Fares, S. Stanton, J. Liddle and G. Gallatin, J. Vac. Sci. Technol., **B18**, 3115 (2000).
14. S.T. Stanton, Proc. SPIE, **4343**, 138 (2001).
15. K. Okamato, K. Suzuki, H. Pfeiffer and M. Sogard, Solid State Technol., **May**, 118 (2000)
16. B.H. Koek, T. Chisholm, A.J. van Run, J. Romijn, J.P. Davey, Microelectronic Engineering, **23**, 81 (1994).
17. M. Mkrtchyan, G. Gallatin, A. Liddle, X. Zhu, E. Munro, W. Waskiewicz, D. Muller, Microelectronic Engineering, **57-58**, 277 (2001).
18. H.I. Smith, J. Vac. Sci. Technol., **B4**, 148 (1986).
19. G.M. Gallatin and J.A. Liddle, Microelecronic Engineering., 46 **365** (1999)
20. S. Tagawa, S. Nagahara, Y. Yamamoto, D. Werst and A.D. Trifunac, Proc. SPIE **3999**, 204 (2000).
21. A. Saeki, T. Kozawa, Y. Yoshida and S. Tagawa, Jpn. J. Appl. Phys. **41**, 4213 (2002)
22. G.M. Gallatin, Proc. SPIE, **4404**, 123 (2001).
23. F.A. Houle, W.D. Hinsberg, M.I. Sanchez and J.A. Hoffnagle, J. Vac. Sci. Technol., **B20**, 924 (2002).
24. W.D. Hinsberg, F.A. Houle, M.I. Sanchez and G.M. Wallraff, IBM J. Res. & Dev. **45**, 667 (2001).
25. L.E. Ocola, Mat. Res. Soc. Symp. Proc., **705**, Y.1.1.1 (2002)
26. F. A. Houle, W. D. Hinsberg, M. Morrison, M. I. Sanchez, G. Wallraff, C. Larson, and J. Hoffnagle, J. Vac. Sci. Technol., **B18**, 1874 (2000).
27. E.H. Anderson, D.L. Olynick, W. Chao, B. Harteneck and E. Veklerov, J. Vac. Sci. Technol., **B18**, 2970 (2000).
28. D.C. Joy, Microelectronic Engineering, **1**, 103 (1983).
29. L.E. Ocola, Microelectronic Engineering, **53**, 433 (2000).
30. D.C. Joy, http://web.utk.edu/~srcutk/htm/interact.htm
31. D.R. Allee, C.P. Umbach and A.N. Broers, J. Vac. Sci. Technol., **B9**, 2838 (1991).
32. J.M. Macaulay "The production of nanometre structures in inorganic materials by electron beams of high current density", Ph.D. dissertation, University of Cambridge (1989).
33. J.M. Macaulay, R.M. Allen, L.M. Brown, S.D. Berger, Microelectronic Engineering, **9**, 57 (1989)
34. A.N. Broers, Proc. R. Soc. Lond. A, **416**, 1 (1988).
35. A.N. Broers, Phil. Trans. R. Soc. Lond. A, **353**, 291 (1995).
36. M. Williamson, A. Neureuther, Proc. SPIE, **3999**, 1189 (2000).
37. M. Sato, L.E. Ocola, A.E. Novembre, K. Ohmori, K. Ishikawa, K. Katsumata and T. Nakayama, J. Vac. Sci. Technol., **B17**, 2873 (1999).
38. K.E. Gonsalves, L. Merhari, H. Wu, and Y. Hu, Advanced Materials, **13**, 703 (2001).